Magnetic Properties and Molecular Structure of Complexes of Substituted Pyrazine Ligands co-ordinated to Iron(II) and Copper(II). Low Dimensional Antiferromagnetic Interactions in Diaquabis(pyrazinecarboxylato)iron(II) †

Cheryl L. Klein and Charles J. O'Connor *
Department of Chemistry, University of New Orleans, New Orleans, Louisiana 70148, U.S.A.
Richard J. Majeste
Department of Chemistry, Southern University in New Orleans, New Orleans, Louisiana 70126, U.S.A.
Louis M. Trefonas
Department of Chemistry, University of Central Florida, Orlando, Florida 32816, U.S.A.

The preparation and magnetic properties at 6—300 K are reported for the complexes $[FeL_2(H_2O)_2]$, $[Fe(HL')_2]\cdot 3H_2O$, and $[Cu(HL')_2]\cdot 3H_2O$, where HL = pyrazinecarboxylic acid and H_2L' = 2,3-pyrazinedicarboxylic acid. The crystal structure of the compound $[FeL_2(H_2O)_2]$ is reported; it crystallizes as a monomer but the crystalline lattice contains an extensive network of hydrogen bonding with the hydrogen bonding along one direction shorter than in other directions. The magnetic data for $[FeL_2(H_2O)_2]$ exhibit a maximum in the temperature-dependent magnetic susceptibility at around 15 K, consistent with the Fisher linear-chain model (J/k = -1.3 K). The complex $[Cu(HL')_2]\cdot 3H_2O$ exhibits no magnetic interaction, whilst $[Fe(HL')_2]\cdot 3H_2O$ shows a low-temperature drop in the effective magnetic moment consistent with a zero-field splitting of the spin $S = 2$ multiplet (D/k = 12.6 K). Crystal data for $[FeL_2(H_2O)_2]$: space group $P2_1/c$, $Z = 2$, a = 5.238(2), b = 11.198(2), c = 10.337(3) Å, β = 100.74(5)°, R = 0.077 for 604 reflections.

We have previously reported structural and magnetic studies of several complexes with substituted pyrazine ligands co-ordinated to copper(II).[1-3] In this report we extend our study of substituted pyrazine ligands to complexes of iron(II). Structural and magnetic studies of iron complexes are not as abundant as studies of copper(II) complexes but the magnetic properties of iron complexes are becoming more familiar.

The structural and magnetic properties of several polymeric iron(II) and iron(III) complexes containing bridging oxalate, squarate [cyclo-$C_4(=O)_2(O^-)_2$],[4] and dihydroxybenzoquinone dianions have been studied.[4-6] Additionally, studies of iron(III) sulphate [7] and iron(III) molybdate [8,9] have been completed indicating a strong magnetic ordering at temperatures less than 20 K. A new series of antiferromagnets of iron(III) with formula $A_2[FeX_5]\cdot H_2O$ ($A = Cs^+$, Pb^+, K^+, or NH_4^+; $X = Cl^-$ or Br^-) have been extensively studied and have been observed to order antiferromagnetically [10] and undergo spin flop transitions in high fields.[11,12]

In our laboratory, we have been studying the effects of substituted pyrazine ligands on the bonding and magnetic properties of bivalent transition metal complexes.[1-3] We have prepared new iron(II) complexes of pyrazinecarboxylic acid (HL) and 2,3-pyrazinedicarboxylic acid (H_2L') and another copper(II) complex of 2,3-pyrazinedicarboxylic acid.

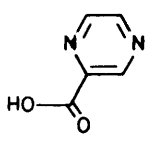

HL

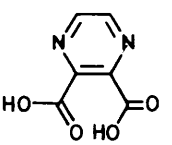

H_2L'

† *Supplementary data available* (No. SUP 23398, 9 pp.): observed and calculated structure factors, thermal parameters, variable-temperature magnetic data. See Notices to Authors No. 7, *J. Chem. Soc., Dalton Trans.*, 1981, Index issue.
Non-S.I. units employed: 1 B.M. = 0.927 × 10^{-23} A m²; 1 e.m.u. = $\frac{1}{4}\pi \times 10^7$ S.I. unit.

Pyrazine is known to be an excellent bridging ligand when co-ordinated to transition metals.[13-23] The use of this relatively simple bridging ligand often permits a study of the interactions of metals over extended distances.

Although the complexes we have prepared do not exhibit direct metal bridging *via* the pyrazine ring, the $[FeL_2(H_2O)_2]$ analogue does exhibit a relatively strong one-dimensional antiferromagnetic interaction propagated *via* a hydrogen-bonded superexchange pathway.

The co-ordination of pyrazinecarboxylic acid to iron(II) results in a monomeric complex which crystallizes in a hydrogen-bonded lattice with stronger hydrogen bonds along one dimension. The co-ordination of 2,3-pyrazinedicarboxylic acid to iron(II) and copper(II) results in apparently isomorphous complexes (consistent with data from the elemental analyses) that did not exhibit magnetic exchange in the measured temperature region. We report on the *X*-ray crystal structure of $[FeL_2(H_2O)_2]$ and powder magnetic susceptibility measurements (from 6 to 300 K) for $[FeL_2(H_2O)_2]$, $[Fe(HL')_2]\cdot 3H_2O$, and $[Cu(HL')_2]\cdot 3H_2O$.

Experimental

Preparation of $[FeL_2(H_2O)_2]$.—A sample of hydrated iron(II) chloride (0.05 mol) was dissolved in water. A sample of pyrazinecarboxylic acid (0.05 mol) was dissolved in hot water (100 cm^3). The two solutions were mixed and crystals were deposited overnight.

Preparation of $[Fe(HL')_2]\cdot 3H_2O$.—A sample of hydrated iron(II) chloride (0.03 mol) was dissolved in enough hot water to form a saturated solution. A stoicheiometric amount of 2,3-pyrazinedicarboxylic acid (0.06 mol) was dissolved in a minimum amount of hot water. The two solutions were mixed and a finely divided purplish black precipitate was deposited overnight (Found: C, 32.5; H, 2.65; Fe, 12.45; N, 12.75; O, 38.8. $C_{12}H_6FeN_4O_8\cdot 3H_2O$ requires C, 32.45; H, 2.7; Fe, 12.6; N, 12.6; O, 39.6%).

Preparation of $[Cu(HL')_2]\cdot 3H_2O$.—A sample of 2,3-pyrazinedicarboxylic acid (0.03 mol) was dissolved in enough

hot water to form a saturated solution. A sample of copper(II) perchlorate (0.03 mol) was dissolved in approximately 20 cm^3 of water. The two solutions were mixed and a finely divided pale blue precipitate deposited immediately (Found: C, 33.0; H, 2.4; Cu, 13.25; N, 13.0; O, 37.75. $C_{12}H_6CuN_4O_8 \cdot 3H_2O$ requires C, 31.9; H, 2.65; Cu, 14.05; N, 12.4; O, 38.95%).

Crystal Structure Determination of $[FeL_2(H_2O)_2]$.—A single crystal of $[FeL_2(H_2O)_2]$ having no dimension greater than 0.35 mm was selected for *X*-ray analysis. The crystal was mounted on a General Electric XRD-490 fully automated diffractometer. Extinctions of the *k* odd for 0*k*0 and *l* odd for *h*0*l* uniquely characterized the space group as $P2_1/c$.

Lattice constants were determined by a least-squares fit * of 25 carefully measured 2θ values under fine conditions (2° take-off angle and 0.05° slit) of the Mo-K_α doublet for reflections with $2\theta > 60°$.

Crystal data. $C_{10}H_{10}FeN_4O_6$, $M = 337.8$, $a = 5.238(2)$, $b = 11.198(2)$, $c = 10.337(3)$ Å, $\beta = 100.74(5)°$, $U = 595.7$ Å^3, $D_m = 1.8 \pm 0.1$ g cm^{-3}, $Z = 2$, $D_c = 1.79$ g cm^{-3}, $F(000) = 344$, space group $P2_1/c$, Mo-K_α radiation ($\lambda = 0.710\ 69$ Å), μ(Mo-K_α) = 12.73 cm^{-1}.

Three-dimensional intensity data were collected by the stationary-crystal, stationary-counter method using balanced zirconium and yttrium filters. A total of 1 311 independent reflections were measured to a 2θ maximum of 52°. Of these reflections, 604 (46%) were considered statistically significant as observed by the criterion $[I_{Zr} - 2\sigma(I_{Zr})] - [I_Y - 2\sigma(I_Y)] > 125$, where the σ's were based entirely on counting statistics. The intensities were corrected for $K_{\alpha_1} - K_{\alpha_2}$ splitting as a function of 2θ, and absorption as a function of φ. Lorentz polarization corrections were made and the intensities were reduced to structure amplitudes in the usual manner.

A preliminary study of the extinction and cell parameters for this complex showed it to be isomorphous with a copper(II) pyrazine complex, $[CuL_2(H_2O)_2]$, described elsewhere.[1] Thus, the initial co-ordinates used for the refinement of $[FeL_2(H_2O)_2]$ were the final co-ordinates found for $[CuL_2(H_2O)_2]$ excluding hydrogen atoms. Refinement of all non-hydrogen atoms using a block-diagonal least-squares program with isotropic temperature factors yielded an *R* value of 0.173. Three missing pyrazine ring hydrogens (calculated on the basis of sp^2 geometry and a C–H bond distance of 1.0 Å) and two water molecule hydrogens found on a difference-Fourier map were added to the co-ordinate list. Continued refinement with anisotropic thermal parameters and an anomalous scattering correction for all non-hydrogen atoms for iron gave $R = 0.085$. Using $1/\sigma^2$ weights, least-squares refinements for the 16-atom structure were continued until the magnitudes of the shifts were less than 0.1 of the estimated standard deviations leading to a final value of $R = 0.077$.

Scattering factors for C, N, O, Cu are taken from ref. 24 and those for hydrogen from ref. 25.

Neither of the complexes of 2,3-pyrazinedicarboxylic acid yielded crystals suitable for crystal structure determination.

Magnetic Measurements.—Magnetic susceptibility data were measured on an alternating force magnetometer (AFM) [1] from 6 to 300 K. The calibration of the instrument and measurement techniques are described elsewhere.[26]

Results

The final fractional atomic co-ordinates for $[FeL_2(H_2O)_2]$ are shown in Table 1. Figure 1 shows a schematic drawing of one monomeric molecular unit with distances and angles indicated with their estimated standard deviations.

Table 1. Fractional atomic co-ordinates with estimated standard deviations in parentheses for $[FeL_2(H_2O)_2]$

Atom	*X/a*	*Y/b*	*Z/c*
Fe	1.000 0(0)	0.500 0(0)	0.500 0(0)
O(8)	1.226 7(17)	0.576 2(6)	0.373 0(9)
O(9)	1.303 6(18)	0.741 9(7)	0.268 2(9)
O(10)	0.692 1(18)	0.471 6(6)	0.334 9(9)
N(1)	0.887 9(21)	0.682 3(7)	0.498 8(12)
N(4)	0.750 8(23)	0.922 9(7)	0.444 8(11)
C(2)	0.990 2(27)	0.748 2(9)	0.407 1(13)
C(3)	0.916 7(28)	0.865 7(10)	0.387 7(14)
C(5)	0.648 9(26)	0.851 0(10)	0.527 1(13)
C(6)	0.716 1(28)	0.738 3(9)	0.559 0(13)
C(7)	1.181 8(26)	0.684 8(9)	0.321 0(0)
H(3)	1.000 0(0)	0.913 0(0)	0.321 0(0)
H(5)	0.508 0(0)	0.889 0(0)	0.572 0(0)
H(6)	0.639 0(0)	0.695 0(0)	0.629 0(0)
H(10)	0.520 0(0)	0.520 0(0)	0.320 0(0)
H(10′)	0.730 0(0)	0.400 0(0)	0.280 0(0)

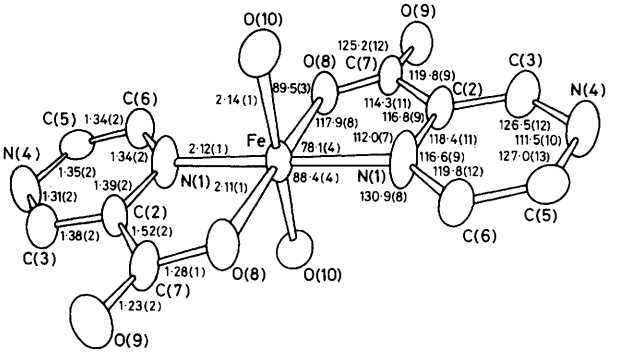

Figure 1. Schematic diagram of the molecular unit of $[FeL_2(H_2O)_2]$ with distances (Å) and angles (°) indicated

Each pyrazinecarboxylic acid ligand has three possible binding positions which may co-ordinate to a metal atom. The ligand is bonded to the metal at two of these positions, N(1) and O(8). The co-ordination sphere is completed by the addition of two axial water molecules which results in a monomeric unit with a distorted octahedral co-ordination sphere. The largest single contribution to the distortion is the O(8)–Fe–N(1) angle of 78.1° caused by the five-membered chelate ring.

The average conjugated C–C bond distance of 1.36 ± 0.02 Å is slightly shorter than the accepted literature value [27] of 1.395 Å while the average conjugated C–N bond distance of 1.35 ± 0.04 Å is slightly longer than the accepted literature value of 1.334 Å. The average of the NCC angles (122.4 ± 4.6°) compares favourably with the literature value of 122.4 ± 1°. The C(7)–O(9) carbonyl bond distance of 1.23 Å is slightly longer than the literature value (1.215 Å) [28] while the C(7)–O(8) distance of 1.28 Å is slightly shorter than the comparable literature value of 1.322 Å.

The magnetic susceptibility measurements were carried out on these complexes in order to determine the extent of the magnetic interactions which were expected to occur. The magnetic data of a polycrystalline sample of $[FeL_2(H_2O)_2]$ and powder samples of $[Fe(HL')_2] \cdot 3H_2O$ and $[Cu(HL')_2] \cdot 3H_2O$ are tabulated in SUP 23398 and are plotted in Figures 2—4. Figure 2 is a plot of magnetic susceptibility as a function

* The conventional reliability index $R = (\Sigma w||kF_o| - |F_c||)/(\Sigma w|kF_o|)$ is cited throughout this paper.

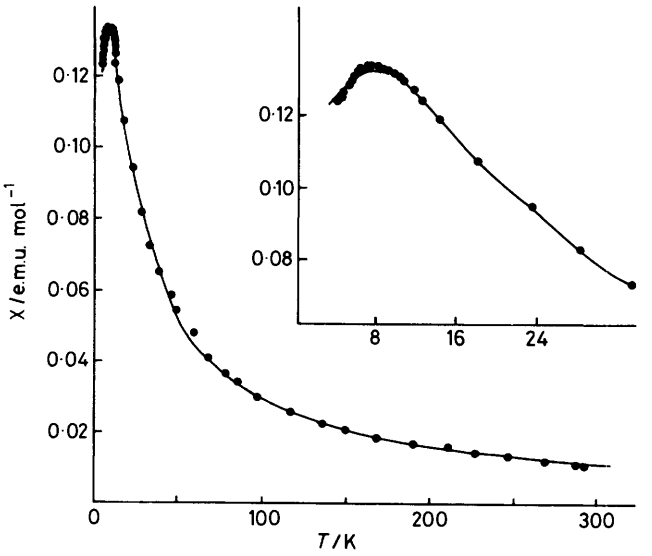

Figure 2. Magnetic susceptibility of $[FeL_2(H_2O)_2]$ plotted as a function of temperature. The inset shows an expanded temperature scale near the maximum in the susceptibility. The line through the points is the best fit of the data as described in text

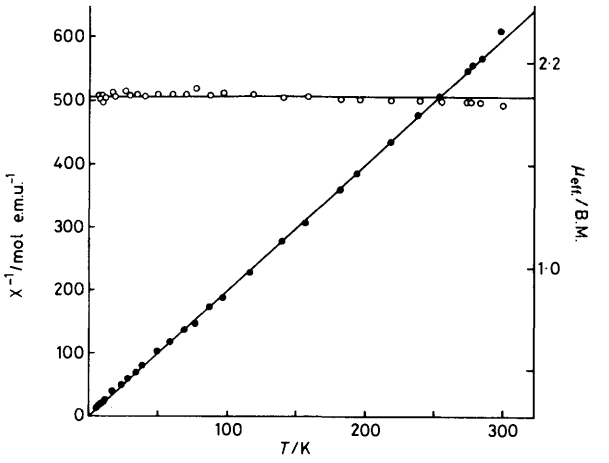

Figure 3. Inverse magnetic susceptibility and effective magnetic moment of $[Cu(HL')_2]\cdot 3H_2O$ plotted as a function of temperature. The line through the points is the best fit of the data as described in text

of temperature. Figures 3 and 4 are plotted as inverse susceptibility and effective magnetic moment as a function of temperature. Since the inverse susceptibility plots are linear as a function of temperature, the Curie–Weiss law [equation (1)] was used to fit the data of the complexes.

$$\chi = \frac{Ng^2\mu_B^2 S(S+1)}{3k(T-\theta)} \qquad (1)$$

The lines through the inverse susceptibility data points in Figures 3 and 4 are the fits of the data to equation (1) with $S = 2$ for iron(II) and $S = \frac{1}{2}$ for copper(II). The fitted parameters are listed in Table 2.

The maximum in the magnetic susceptibility plot of $[FeL_2(H_2O)_2]$ shown in Figure 2 is consistent with short-range magnetic ordering. There is no exact solution to the Van Vleck equation for a one-dimensional magnetic chain;

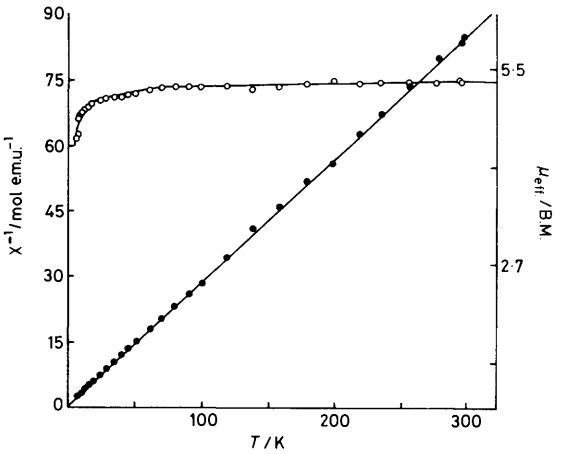

Figure 4. Inverse magnetic susceptibility and effective magnetic moment of $[Fe(HL')_2]\cdot 3H_2O$ plotted as a function of temperature. The line through the points is the best fit of the data as described in text

however, the Fisher linear-chain model [29] [equation (2)] for the magnetic susceptibility is often used in fits of magnetic data for systems with spin $S = 2$. Since $[FeL_2(H_2O)_2]$ is a hydrogen-bonded linear chain, the magnetic data were fitted to the Fisher model. The result of this fit is shown as the smooth curve through the magnetic susceptibility data points in Figure 2 with the parameters listed in Table 2. The observation of the maximum in the plot of the temperature-dependent magnetic susceptibility is indicative of relatively strong antiferromagnetic coupling. The Van Vleck equation is shown by equation (2) where $U = T/T_0 - \coth(T_0/T)$ and $T_0 = 2JS(S+1)k$; J is the intrachain coupling parameter.

$$\chi = \frac{Ng^2\mu_B^2 S(S+1)}{3kT} \cdot \frac{1-U}{1+U} \qquad (2)$$

For the non-hydrogen-bonded iron(II) complex, $[Fe(HL')_2]\cdot 3H_2O$, we believe the slight decrease in magnitude of the effective magnetic moment as T approaches 0 K is the result of a zero-field splitting of the spin multiplet (D). The magnetic susceptibility equations (3) for zero-field splitting of the spin multiplets were derived from the Van Vleck equation with $S = 2$, where $C = Ng^2\mu_B^2/kT$ and $x = D/kT$. The

$$\chi_{\parallel} = C\frac{2e^{-x} + 8e^{-4x}}{1 + 2e^{-x} + 2e^{-4x}}$$
$$\chi_{\perp} = C\frac{\frac{6}{x}(1 - e^{-x}) + \frac{4}{3x}(e^{-x} - e^{-4x})}{1 + 2e^{-x} + 2e^{-4x}} \qquad (3)$$

line through the data points for the effective magnetic moment in Figure 2 is the fit of the data to the powder magnetic susceptibility equation $[\chi_p = (\chi_{\parallel} + 2\chi_{\perp})/3]$ using the zero-field splitting term. The fitted parameters are listed in Table 2. For the sake of completion, the parameters which result from a fit of the magnetic data of $[Fe(HL')_2]\cdot 3H_2O$ to the Fisher linear-chain model are also included in Table 2. A suitable fit of the magnetic data of $[FeL_2(H_2O)_2]$ to the crystal field model could not be obtained.

Discussion

Results from the X-ray crystal structure determination of $[FeL_2(H_2O)_2]$ show an extensive hydrogen-bonding network

Table 2. Magnetic parameters for $[Fe(HL')_2]\cdot 3H_2O$, $[FeL_2(H_2O)_2]$, and $[Cu(HL')_2]\cdot 3H_2O$

Compound	g	θ/K	Jk^{-1}/K	Dk^{-1}/K	Model
$[Fe(HL')_2]\cdot 3H_2O$	2.16(2)	−2.2(2)			$S = 2$ Curie–Weiss
	2.14(2)		−0.2(1)		$S = 2$ Fisher chain
	2.16(2)			12.6(2)	$S = 2$ Zero-field splitting
$[FeL_2(H_2O)_2]$	2.13(2)	−11.7(5)			$S = 2$ Curie–Weiss
	2.12(2)		−1.3(1)		$S = 2$ Fisher chain
$[Cu(HL')_2]\cdot 3H_2O$	2.32(2)	−0.2(2)			$S = \frac{1}{2}$ Curie–Weiss

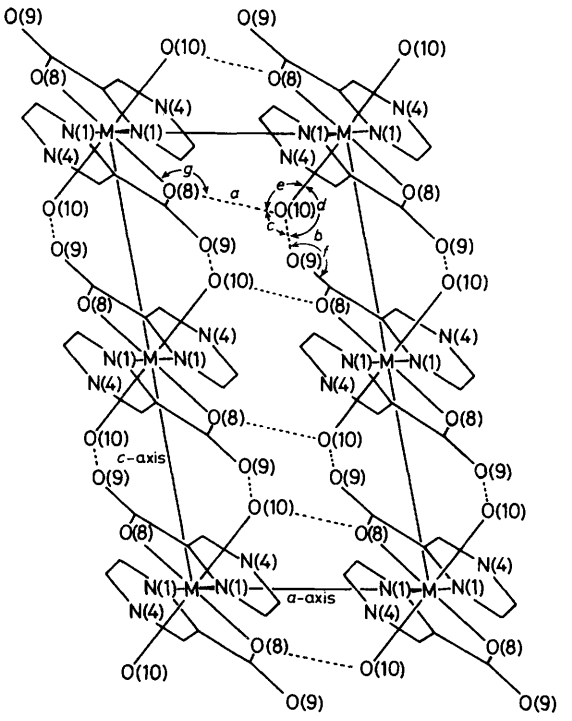

Figure 5. Projection of the $[FeL_2(H_2O)_2]$ lattice in the *ac* plane. The hydrogen-bonding contacts are illustrated by a dotted line. Interaction distances and angles are listed in Table 3

within the unit cell. The hydrogen bonding is illustrated schematically in Figure 5. There are two distinct types of hydrogen bonds. The shorter H-bond pathway involves O(10) · · · O(8) hydrogen bonding and a simple Fe–OH · · · O–Fe bridge. This H–bond pathway generates a one-dimensional chain along the *a* axis. The secondary H–bond pathway consists of O(10) · · · O(9) contacts which are propagated along (011) and (0$\bar{1}$1) to complete the three-dimensional interaction. This secondary hydrogen bonding involves a five atom (Fe–OCO · · · HO–Fe) rather than a three atom bridge, and is therefore expected to have a smaller contribution to the overall magnetic exchange. These interaction distances and angles as well as other pertinent hydrogen-bonding distances and angles are listed in Table 3.

The magnetic data for $[Cu(HL')_2]\cdot 3H_2O$ show no magnetic exchange interaction. The effective magnetic moment appears to be invariant as a function of temperature (Figure 3) indicative of a classical paramagnet following Curie law. The magnetic data for $[Fe(HL')_2]\cdot 3H_2O$ show a slight decrease in the effective magnetic moment as the temperature approaches 0 K. We were not able to obtain structural data for either of the dicarboxylic acid complexes so it is unknown

Table 3. Pertinent hydrogen-bond distances (Å) and angles (°) for $[FeL_2(H_2O)_2]$ illustrated in Figure 5

$a = 2.80$, $b = 2.79$, $c = 120.6$, $d = 112.5$, $e = 111.9$, $f = 138.4$, $g = 121.7$

O(10)–H(10)	1.04
O(10)–H(10′)	1.03
O(8)–H(10)	1.83
O(9)–H(10′)	1.84
H(10)–O(10)–H(10′)	125.0
O(8)–H(10)–O(10)	152.5
O(9)–H(10′)–O(10)	152.2

whether the drop in the effective magnetic moment of $[Fe(HL')_2]\cdot 3H_2O$ is due to intermolecular or intramolecular interactions. Reasonably good fits of the magnetic data for $[Fe(HL')_2]\cdot 3H_2O$ may be obtained using either a model including a zero-field splitting term or a Fisher linear-chain model. Since both iron(II) salts have copper(II) analogues with identical atomic composition, and since the two complexes which allow structural studies {*i.e.* $[ML_2(H_2O)_2]$; M = Fe^{2+} or Cu^{2+}} are isomorphous,[1] it is likely that the structure of the dicarboxylate analogues {$[M(HL')_2]\cdot 3H_2O$; M = Fe^{2+} or Cu^{2+}} are also very similar. In the light of the lack of exchange in the analogous $[Cu(HL')_2]\cdot 3H_2O$ complex we believe the low-temperature magnetic behaviour in $[Fe(HL')_2]\cdot 3H_2O$ is occurring in the absence of significant magnetic exchange and is due to the effects of crystal-field splitting of the spin $S = 2$ multiplet.

If there is a detectable crystal-field splitting of the iron(II) spin multiplet in $[Fe(HL')_2]\cdot 3H_2O$, it is likely that crystal-field splitting is also present in the similar co-ordination fields of the complex $[FeL_2(H_2O)_2]$. For this reason, the value of the coupling parameter is assigned an error limit which is larger than the statistically calculated value. It is useful to point out, however, that the characteristic maximum of a linear-chain model cannot be mimicked by a crystal-field splitting model. When the crystal-field splitting parameter is large (*i.e.* $D \gg kT$), the powder magnetic susceptibility $[(\chi_{\parallel} + 2\chi_{\perp})/3]$ does not decrease but maintains a constant value as the temperature is lowered.

It is also interesting to point out that the magnetic exchange in the isomorphous hydrogen-bonded complexes of formula $ML_2(H_2O)_2$ is antiferromagnetic for M = Fe^{2+} and is ferromagnetic [1] for M = Cu^{2+}. This is undoubtedly due to the availability of a greater number of half-filled orbitals in the iron(II) complex. For copper(II), the single unpaired electron is expected to be in the d_{x2-y2} orbital. Iron(II), on the other hand, has four unpaired electrons. As a result of the iron(II) electron configuration, a greater number of overlap pathways are available to propagate antiferromagnetic exchange. Anderson [30] has proposed that the orientation of the electronic orbitals in the bridge between magnetically coupled metals will determine the nature of the coupling. A pathway which has a positive overlap of the orbitals will propagate anti-

ferromagnetic exchange, while a pathway which contains an orthogonal overlap will propagate ferromagnetic exchange. Copper(II) and iron(II) have differences in the orbital occupancy of unpaired electrons and therefore a difference in the nature of the magnetic exchange is not unexpected.

References

1 C. L. Klein, R. J. Majeste, L. M. Trefonas, and C. J. O'Connor, *Inorg. Chem.*, 1982, **21**, 1891.
2 C. L. Klein, L. M. Trefonas, C. J. O'Connor, and R. J. Majeste, *Cryst. Struct. Commun.*, 1981, **10**, 891.
3 C. J. O'Connor, C. L. Klein, R. J. Majeste, and L. M. Trefonas, *Inorg. Chem.*, 1982, **21**, 64.
4 J. T. Wrobleski and D. B. Brown, *Inorg. Chem.*, 1979, **18**, 2738.
5 J. T. Wrobleski and D. B. Brown, *Inorg. Chem.*, 1979, **18**, 498.
6 S. S. Barros and S. A. Freidberg, *Phys. Rev.*, 1966, **141**, 637.
7 G. J. Long, G. Longworth, P. Battle, A. K. Cheetham, R. V. Thundathil, and D. Beveridge, *Inorg. Chem.*, 1979, **18**, 624.
8 M. H. Rapposch, J. B. Anderson, and E. Kostiner, *Inorg. Chem.*, 1980, **19**, 3531.
9 G. J. Long, G. Longworth, P. Bottle, A. K. Cheetham, R. V. Thundathil, and D. Beveridge, *Inorg. Chem.*, 1979, **18**, 624.
10 R. L. Carlin, C. J. O'Connor, and S. N. Bhatia, *J. Am. Chem. Soc.*, 1977, **99**, 7728.
11 C. J. O'Connor, B. S. Deaver, jun., and E. Sinn, *J. Chem. Phys.*, 1979, **70**, 5161.
12 F. Palacio, A. Paduan-Filho, and R. L. Carlin, *Phys. Rev. B*, 1980, **21**, 296.
13 C. Creutz and H. Taube, *J. Am. Chem. Soc.*, 1969, **91**, 3988; 1973, **95**, 1086.
14 J. K. Beattie, N. S. Hush, and P. R. Taylor, *Inorg. Chem.*, 1976, **15**, 992.
15 T. J. Meyer, M. J. Powers, D. J. Salmon, and R. W. Callahan, *J. Am. Chem. Soc.*, 1977, **99**, 1064.
16 T. J. Meyer, *Acc. Chem. Res.*, 1978, **11**, 94.
17 J. A. Baumann, D. J. Salmon, S. T. Wilson, and T. J. Meyer, *Inorg. Chem.*, 1979, **18**, 2472.
18 P. W. Charreck, M. Goldstein, E. M. McPartlin, and W. E. Unsworth, *Chem. Commun.*, 1971, 1634.
19 M. Inoue and M. Kubo, *Coord. Chem. Rev.*, 1976, **21**, 1.
20 H. W. Richardson, J. R. Wasson, and W. E. Hatfield, *Inorg. Chem.*, 1977, **16**, 484.
21 A. B. Blake and W. E. Hatfield, *J. Chem. Soc., Dalton Trans.*, 1978, 868.
22 M. S. Haddad, D. N. Hendrickson, J. P. Cannady, R. S. Drago, and D. S. Bieckza, *J. Am. Chem. Soc.*, 1979, **101**, 898.
23 J. Darriet, M. S. Haddad, E. N. Duesler, and D. N. Hendrickson, *Inorg. Chem.*, 1979, **18**, 2679.
24 D. T. Cromer and J. T. Waber, *Acta Crystallogr.*, 1965, **18**, 104.
25 ' International Tables for *X*-Ray Crystallography,' Kynoch Press, Birmingham, 1968, vol. 3.
26 C. J. O'Connor, *Prog. Inorg. Chem.*, 1982, **29**, 203.
27 ' Tables of Interatomic Distances and Configuration in Molecules and Ions,' Spec. Publ. No. 11, The Chemical Society, London, 1958, Supplement (1964).
28 ' Molecular Structures and Dimensions; Interatomic Distances,' N. V. A. Oosthoek's Uitgevers Mij, Utrecht, vol. A1, 1960—1965.
29 M. E. Fisher, *Am. J. Phys.*, 1964, **32**, 343.
30 P. W. Anderson, *Phys. Rev.*, 1950, **79**, 350.

Received 25*th February* 1982; *Paper* 2/347